lubricants

Article

Experimental Study on the Influence of Stearic Acid Additive on the Elastohydrodynamic Lubrication of Mineral Oil 2137

Wei Li, Feng Guo *, Chenglong Liu and Zhaoqun Ma

School of Mechanical & Automotive Engineering, Qingdao University of Technology, Qingdao 266520, China; shlw@qut.edu.cn (W.L.); liuchenglong@qut.edu.cn (C.L.); mzq8135@163.com (Z.M.)
* Correspondence: mefguo@qut.edu.cn; Tel.: +86-13863945503

Abstract: Using an optical elastohydrodynamic lubrication (EHL) test rig, oil film thickness and the coefficient of friction (COF) were measured, and the influence of stearic acid additive on the EHL performance of mineral oil 2137 was investigated. The results showed that 2137 with 0.3 wt% stearic acid (denoted to as 2137s) achieved the same film thickness as 2137, while the COF of 2137s was significantly lower than that of 2137 when the contact was under conditions of a fully lubricant supply. Under conditions of limited lubricant supply, 2137 base oil was prone to oil starvation with the increase of entrainment velocity. On the other hand, 2137s significantly mitigated the oil starvation. This was attributed to the fact that lower surface energy by the adsorption of stearic acid results in discontinuous oil-droplet distribution on the lubrication track and, therefore, early pressure generation. Moreover, it is interesting to find that less 2137s supply quantity can produce higher film thickness when the contact is at high speeds, which is attributed to the fact that a smaller quantity of 2137s gives smaller droplets on the lubrication track, and the resultant small surface area–volume ratio presents oil more resistance to the centrifugal force and results in less oil escaping from the lubrication track. The addition of stearic acid reduced the average COF of 2137 mineral oil by about 13.3%

Keywords: oiliness additives; film thickness; coefficient of friction; limited lubricant supply; surface absorb

check for updates

Citation: Li, W.; Guo, F.; Liu, C.; Ma, Z. Experimental Study on the Influence of Stearic Acid Additive on the Elastohydrodynamic Lubrication of Mineral Oil 2137. *Lubricants* **2023**, *11*, 446. https://doi.org/10.3390/lubricants11100446

Received: 21 September 2023
Revised: 11 October 2023
Accepted: 14 October 2023
Published: 16 October 2023

1. Introduction

Lubrication is the most effective way to reduce friction and wear of mechanical components, extend equipment life, and reduce energy consumption, and choosing the appropriate lubrication method is particularly important [1]. With the increasing demand for environmental protection and energy conservation, precise lubrication has been receiving more attention [2,3] in the tribology community. Limited lubricant supply (LLS) has become one of the important methods in lubrication design, where the oil supply quantity is limited in such a way that an optimal lubrication status can be achieved. However, when LLS applied oil starvation at the inlet of a contact and this could not be avoided, strategies have to be found to improve the oil replenishment on the lubrication track. Wedeven et al. [4] first reported the elastohydrodynamic lubrication (EHL) under oil-starved conditions using optical interferometry and provided a formula to describe the relationship between the entrance distance (the distance between the entrance supply bend boundary and the contact zone boundary) and the reduction in film thickness. Guangteng and Kingsbury [5,6] conducted optical EHL tests with different lubricants and found that when oil starvation occurred, the lubricating film thickness is reduced to an approximately constant thickness of tens of nanometers, which was independent of speed. Fischer et al. [7] determined the characteristic rotational speed that leads to starvation based on the composition of the lubricating grease. Cann et al. [8] studied the transition between fully flooded and oil-starved conditions in EHL using a ball-on-disc test and developed a parameter to identify the onset of oil starvation, which involves oil quantity, viscosity, speed, and load. Maruyama et al. [9] examined the relationship between the supplied oil flow rate and oil film thickness under steady starved lubrication. Recently, Ebner et al. [10] studied LLS lubrication through a twin-disc test, showing that a very small amount of lubricating oil is sufficient for lubrication, achieving EHL under high loads.

It is particularly important to maximize the effectiveness of a limited quantity of lubricant in LLS, and current methods include surface texturing [11–13], surface chemical modification [14,15], and the addition of oil-soluble additives [16,17]. In terms of surface texture, Niu et al. [11] prepared a series of shallow concave textured surfaces with different geometric parameters (area density, diameter, and depth) on the surface of medium carbon steel and conducted friction and wear tests. They found that the surface with the best texture depth can effectively extend the steady-state and reduce friction and wear in the changing state, thus achieving a longer sliding distance under the condition of oil starvation lubrication. Matthew et al. [12] designed and employed laser surface texturing techniques to fabricate a set of dimples characterized by a circular cross-section and conical profile. When these textures are strategically positioned outside the contact footprint track yet in close proximity to the disc, they demonstrate a reduction in both the coefficient of friction and wear. Hirayama et al. [13] experimentally studied the laser processing groove outside the contact zone under the condition of point-contact elastohydrodynamic lubrication (EHL) and studied its influence on the thickness of the lubrication film. It was found that the groove depth and angle were the key parameters to determine the oil film thickness because they control the amount of lateral oil leakage at the contact point. In terms of surface chemical modification, Li et al. [14] adjusted the distribution of oil pools on both sides of the contact region by constructing a wettability gradient, which was generated by an oil–wet trajectory surrounded by two oil-repellent regions on the solid surface. Liu et al. [15] constructed an oil-hydrophilic lubricating track bounded by an oil-phobic region on the friction surface through surface chemical modification. Under the condition of limited oil supply, step wettability can improve the oil supply effect on the contact track and increase the thickness of the lubricating oil film. All these methods provide ideas for the active control of the spent oil lubrication state produced in the friction process.

Additives play an important role in improving the performance of lubricating oils [18–22]. Oiliness agents or friction modifiers, as important members of additives, can effectively enhance the anti-friction properties of lubricating oils. The study of oiliness agents began in 1918 when Wells et al. [23] dissolved low-concentration plant oil-derived free fatty acids in mineral oil and found that it improved the anti-friction and anti-wear effects of mineral oil. Doig et al. [24,25] used molecular dynamics simulations to investigate the adsorption behavior of stearic acid on iron oxide surfaces, revealing the significant impact of oiliness additives on friction performance. Fry et al. [26] studied the adsorption phenomenon of oiliness additives in hexadecyl oil on silicon surfaces and confirmed the positive role of the adsorption layer in improving contact friction. Most of the aforementioned studies focused on improving boundary lubrication conditions, but oiliness additives also have significant effects under EHL conditions. Kalin et al. [27] selected several simple oiliness additives (amines, alcohols, amides, and fatty acids) and reduced the friction coefficient under elastohydrodynamic lubrication in steel/steel contacts, indicating application potential of oiliness additives in elastohydrodynamic lubrication. Zang et al. [28] conducted experiments on slider-on-disc contact LLS lubrication and found that the formation of discrete oil droplets on the weakly wetted surface created by ionic liquid additives facilitated the bearing of the lubricating oil film. Li et al. [29] also demonstrated through numerical calculations that, under LLS conditions, discontinuous oil droplets caused by differences in surface wetting could enhance the lubrication of sliding bearings. The aforementioned studies indicate that oiliness agents, by adsorbing onto tribo-surfaces and forming thin films with low surface energy, effectively decrease the friction of lubrication films.

In summary, existing research is mostly focused on the impact of oiliness additives on synthetic oil in boundary lubrication performance, with limited studies on the effect of stearic acid additives on EHL performance. Therefore, in this study, by adding stearic acid to mineral oil 2137 and utilizing a light interference lubricating film measurement system, the influence of stearic acid additives on the lubricating performance of mineral oil 2137 was investigated.

2. Experimental

2.1. Experimental Apparatus and Scheme

The experiment for measuring the film thickness and COF was conducted using a self-developed optical elastohydrodynamic lubrication test rig in the authors' laboratory. During the experiment, both the interference images and the COF were simultaneously acquired. The structure of the rig is shown in Figure 1. The speeds of the glass disc and the steel ball could be set separately, allowing for different SRR tests. The film thickness measurement utilized the principle of optical interference. Red (wavelength 640 nm) laser and green (wavelength 525 nm) laser were employed. Interference fringes were obtained by multiple reflection and refraction of the red and green lasers, which were then captured by a CCD camera after magnification by a microscope. The captured images were processed by the dichromatic intensity modulation approach (DIIM) [30] to obtain the profile of the oil film. The measurement of the friction force was realized by a force sensor in contact with one end of a lever with the ball-drive unit and loading weights. The signal was transmitted to the computer through a data acquisition card. Oil film interferogram and friction coefficients were acquired simultaneously. Under each working condition, the steel ball and glass disk were set to run steadily for 1 min, during which the interference pattern was randomly saved and the friction coefficient was recorded synchronously through pulse triggering.

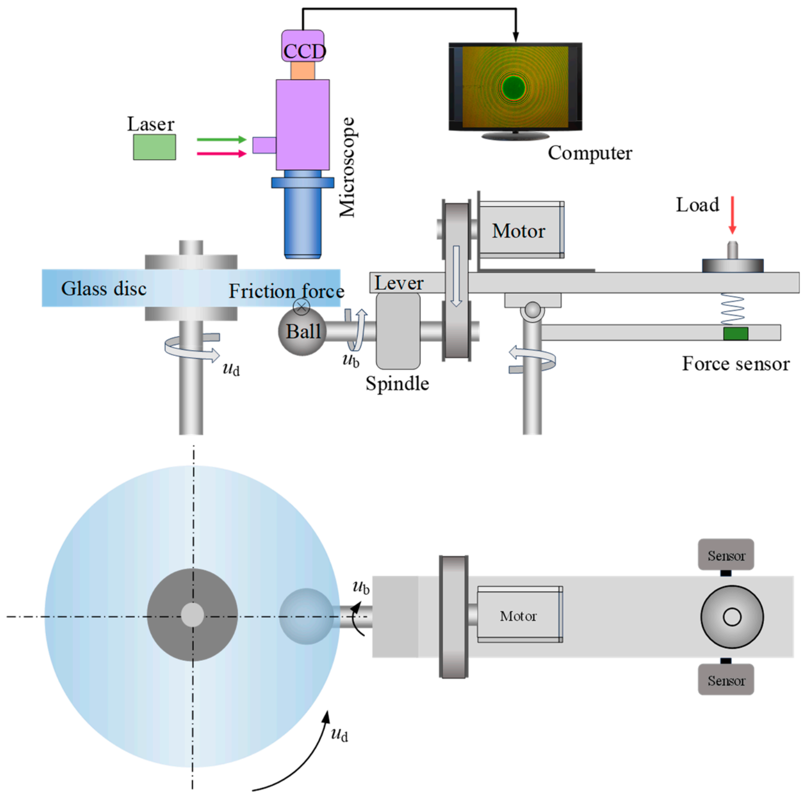

Figure 1. Schematic diagram of optical elastohydrodynamic lubrication test rig.

2.2. Experimental Conditions and Materials

Two lubricants were used in the experiments. One was 2137 base oil. 2137 is a refined mineral oil, which is a type II mineral oil similar to 500 N, and its main components are alkane compounds. The other was 2137s, which was 2137 base oil with 0.3 wt% stearic acid ($C_{18}H_{36}O_2$). As shown in Figure 2, the preparation process of 2137s was as follows. Firstly, 0.3 g stearic acid powder was added to 99.7 g 2137 base oil. The mixture was stirred for two hours at 60 °C to fully dissolve the stearic acid. After heating, the solution was cooled and left to stand at room temperature for two days. It was observed that the solution was transparent, homogeneous, and no substance precipitated, indicating full dissolution of stearic acid in 2137 base oil. The properties of the two lubricants are listed in Table 1.

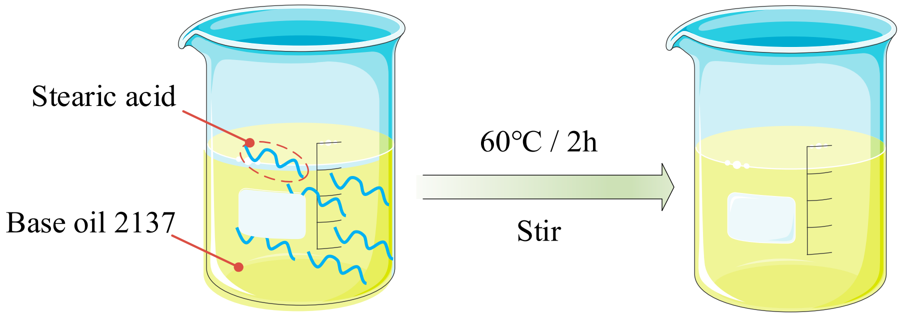

Figure 2. Preparation of the 2137s solution.

Table 1. Properties of lubricants used.

Lubricant	Dynamic Viscosity (mPa·s @22 °C)	Refractive Index
2137	220.8	1.475
2137s	199.8	1.475

The glass disc material was BK7 glass. In order to improve the imaging quality, a thin chromium (Cr) film with a thickness of about 20 nm was coated on the contact surface of the glass disc. The roughness of the glass disc was Ra = 4 nm. The ball was made of AISI 521000 steel with a diameter of 25.4 mm and a surface roughness of Ra = 14 nm. The radius of the circular trajectory was 60 mm. The experimental conditions are shown in Table 2. The slide-roll-ratio (SRR) is defined as SRR = $(u_a - u_b)/u_e$, where $u_e = (u_a + u_b)/2$ is the entrainment velocity, and u_a and u_b are the linear velocities of the contact point on the disc and the ball, respectively. In the LLS test, a micropipette was used for quantitative oil supply. Before starting the experiment, the ball and the disc were brought into approximate contact. The lubricant was evenly distributed on the contact track of the glass disc, and a 10-min pre-running was performed.

Table 2. Conditions of the experiments.

Condition	Value
Volume of the oil supply, $V/\mu L$	5, 10, 20, Fully flooded (1 mL)
Load, w/N	15, 30
Entrainment velocity, $u_e/mm{\cdot}s^{-1}$	1–512
Slide-roll-ratio, SRR	0.1, 0.2, 0.4, 0.6, 0.8, 1.0
Temperature, $T/°C$	22 ± 1
Relative humidity, RH/%	50 ± 5

3. Results and Discussion

3.1. The Effect of Stearic Acid on the 2137 Mineral Oil under Fully Flooded Condition

Under fully flooded conditions, Figure 3 shows the variation curves of film thickness and COF with entrainment velocity for a load of 30 N and an SRR of 0.1 for two lubricants. From the graph, it can be observed that the film thickness of both 2137 and 2137s lubricants increased with increasing entrainment velocity, and there was not significant difference between their film thickness. It is worth noting that under the same test conditions, the COF of 2137s was significantly lower than that of the 2137 base oil. This is mainly because stearic acid in 2137s can form an adsorption film on the contacting surface during the lubrication process. The formed adsorption film and the fluid film have a certain degree of slippage between them, thereby reducing the COF. The COF of both lubricants shows decreased followed by an increase with increasing speed. At lower speeds, the oil film thickness was low, and the contact zone was in the mixed lubrication stage with contact of rough peaks. As the speed increased, the oil film thickness increased, the lubrication state improved, and the contact of rough peaks decreased, resulting in a continuous decrease in COF. When the speed continued to increase, the lubrication state entered the fluid lubrication stage, where the COF mainly came from the shear within the fluid. Moreover, the higher the speed, the greater the shear force within the fluid, resulting in an increase in COF. The friction versus speed in Figure 3 is correlated well to the Stribeck curve.

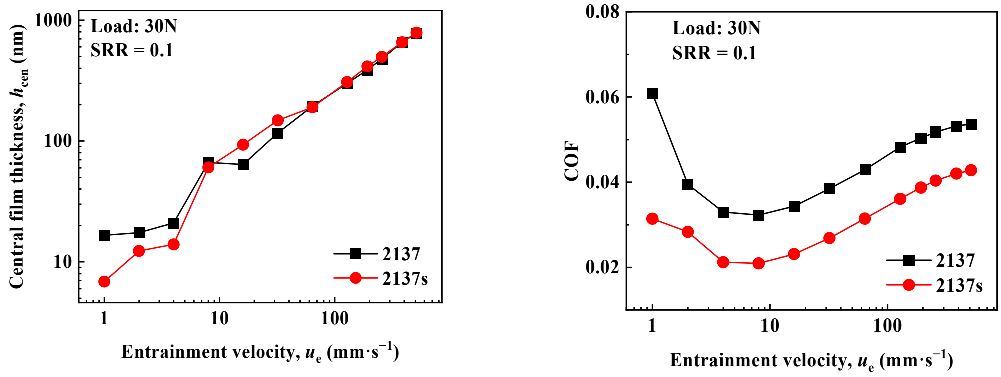

(**a**) (**b**)

Figure 3. Variation curves of film thickness and COF vs. entrainment velocity for 2137 and 2137s: (**a**) central film thickness vs. u_e; (**b**) COF vs. u_e.

Figure 4 shows the variation of the COF of 2137 and 2137s with the entrainment velocity under different SRRs. It can be seen from the curves at lower SRRs (0.1, 0.2), the COF of 2137 and 2137s both show a trend of first decreasing and then increasing with the increase of the entrainment velocity, which is consistent with the general Stribeck curve. At higher SRRs (0.4, 0.6, 0.8, 1), nevertheless, the COF of 2137 and 2137s varied differently. With the increase of the entrainment velocity, the COF of 2137 and 2137s showed a trend of decreasing, then increasing, and then decreasing again. Under a large SRR, when the entrainment velocity was high, the COF showed a significant decrease, and the larger the SRR and entrainment velocity, the more obvious the decreasing trend of the COF. This is because under the condition of a higher SRR, when the entrainment velocity is high, both lubricants, 2137 and 2137s, exhibit obvious thermal thinning and shear thinning effects, which weaken the fluid shear in the contact area and thus reduce the COF in the contact area. To investigate the influence of the SRR on the effect of stearic acid additive, the average value of COF within the range of entrainment velocity of 1–384 mm/s under different SRRs was calculated, as shown in Figure 4c. It can be seen from the figure that the COF of both lubricants increases with the increase of the SRR, which is because the increase in the SRR leads to the increase of the shear at the friction interface, and hence increase in COF. Moreover, the COF of 2137s is significantly lower than that of 2137, mainly due to the adsorption of stearic acid on the friction surface. This friction-reduction performance is more pronounced at lower SRRs, mainly because the damage to the adsorption film is weaker at lower SRRs, while the adsorption film may be damaged to a certain extent at higher SRRs, resulting in a weakening of the friction-reducing effect.

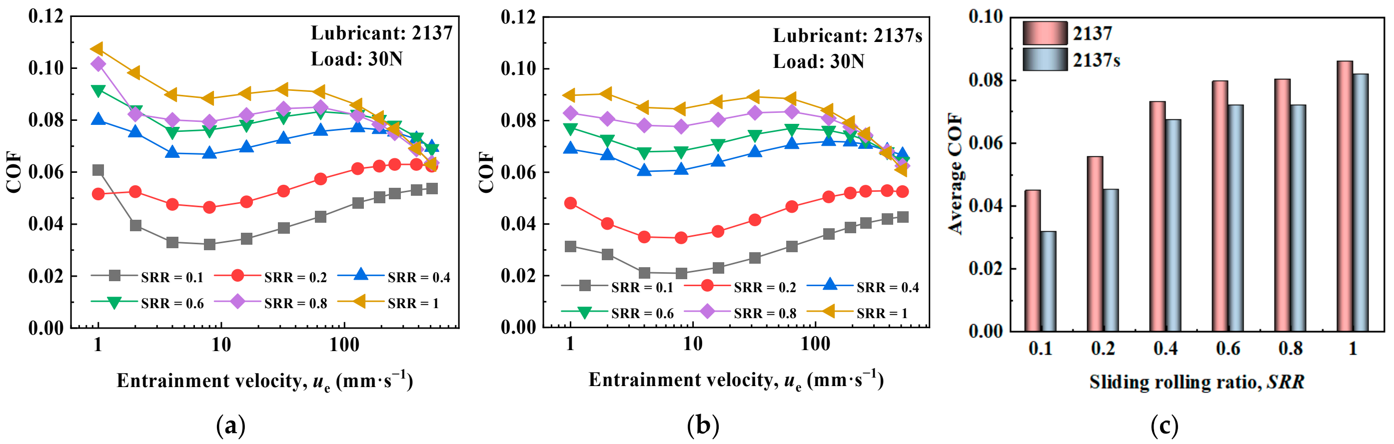

Figure 4. Variation of the COF of 2137 and 2137s: (**a**) COF vs. u_e, 2137; (**b**) COF vs. u_e, 2137s, 30 N; (**c**) average COF of 2137 and 2137s.

The COF variation with the sliding–rolling ratio under different entrainment velocities was studied. Figure 5 shows the curves of COF with SRR for two lubricants under three entrainment velocities under sufficient oil supply conditions. When SRR was less than 0.4, the increase of COF with SRR for the lubricant followed a linear law approximately, indicating a Newtonian fluid behavior. As the SRR increased, when SRR was greater than 0.6, lubricants showed different friction behaviors at different entrainment velocities. At entrainment velocities of 64 mm/s and 192 mm/s, with the increase of SRR, COF showed a slight increase at an entrainment velocity of 512 mm/s. When SRR was greater than 0.6, both 2137 and 2137s exhibited a significant decrease in COF vs. SRR. At higher entrainment velocities and larger SRRs, the lubricant is affected by the combined effects of shear thinning and thermal effects.

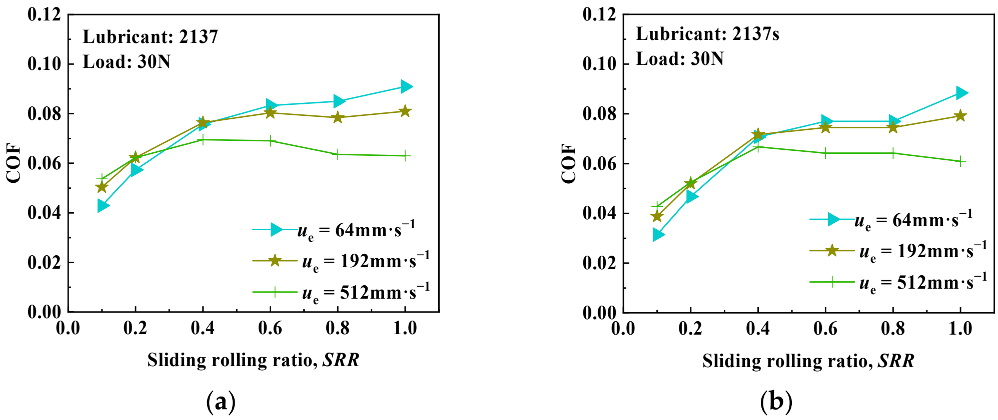

Figure 5. COF varies with SRR.: (**a**) 2137, 30 N; (**b**) 2137s, 30 N.

When the SRR is 0.1, the film thickness and COF of 2137 base oil under fully flooded conditions was measured at loads of 15 N and 30 N, as shown in Figure 6. From Figure 6a, it can be observed that the film thickness curves presented by 15 N and 30 N are relatively close, indicating that the film thickness does not have marked dependence on load, which is the intrinsic characteristics of elastohydrodynamic lubrication. In contrast to film thickness, the influence of load on COF is more pronounced. The COF corresponding to the 30 N load is significantly higher than that of the 15 N load. This is mainly because the increase in load leads to an increase in the oil film pressure within the contact zone, enhancing the viscosity and shear force in the contact zone and causing a noticeable increase in COF. Furthermore, from Figure 6b, it can be observed that as the load increases, the speed decreases at which the COF starts to rise.

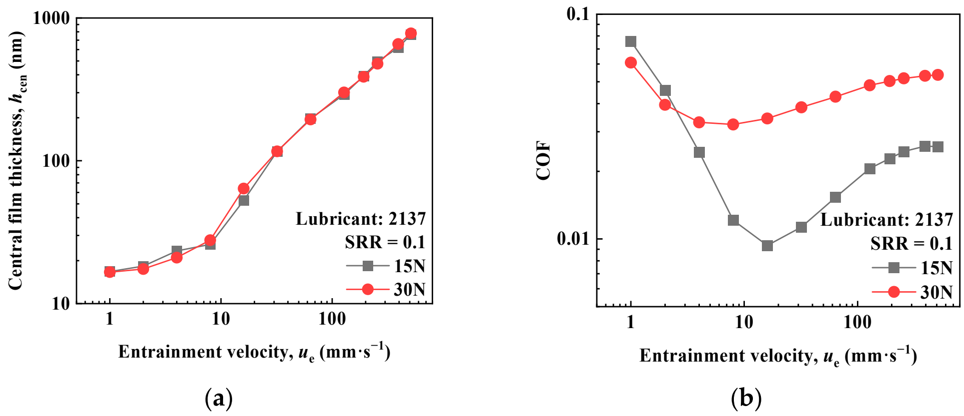

Figure 6. Film thickness and COF versus speed, 2137 base oil under loads of 15 N and 30 N: (**a**) Central film thickness vs. u_e; (**b**) COF vs. u_e.

3.2. Influence of Stearic Acid under Limited Lubricant Supply Conditions

In practical engineering, excessive lubrication is often used for mechanical components, which can sometimes be detrimental to the operation of the machine. A small amount of lubricant is sufficient to achieve effective lubrication for tribo-pairs such as air-oil lubrication in high-speed bearings, which can avoid temperature rise by oil churning. Therefore, this section studies the influence of stearic acid on the tribology performance of base oil 2137 under limited oil supply conditions. Figure 7 shows the influence of oil supply amount on the central oil film thickness of the two lubricants with a load of 15 N and a SRR of 0.1. From Figure 7a–c, it can be observed that the central film thickness of the base oil 2137 first increases and then decreases, and there exists a critical speed where the film thickness starts to decrease. This critical speed represents the transition of the lubrication from adequate oil supply to insufficient oil supply. When the oil supply amount is 5 µL, the critical speed of 2137 is 64 mm/s. When the speed exceeds the critical speed, the central film thickness of 2137 decreases significantly. When the oil supply amount reaches 10 µL, the critical speed is 128 mm/s, and when the oil supply amount is 20 µL, the critical speed is 256 mm/s. With the increase in oil supply amount, the critical speed of the base oil continues to rise, indicating that increasing the oil supply amount can effectively improve the lubrication. From Figure 7d, it can be seen that under sufficient oil supply, the central film thickness increases with increasing speed. Under limited oil supply, the measured film thickness of 2137s presents better film formation behavior than that of the base oil 2137. Therefore, under limited oil supply conditions, 2137s can improve the oil supply and lubrication state within a certain range of operating conditions.

To investigate the influence of stearic acid on the oil film thickness shown in Figure 7, Figure 8 gives the entrance oil pool of the two oils at various oil supply amounts (5 µL, 10 µL, 20 µL, and full flooded) under various entrainment velocities. The dashed line in the figure indicates the oil–air meniscus boundary in the entrance region, and the distance from the meniscus boundary to the contact center reflects the degree of oil depletion. From Figure 8a, it can be observed that when the volume of oil supply is 5 µL, the 2137 base oil exhibits obvious oil depletion, and this depletion phenomenon intensifies with increasing entrainment velocity. When the entrainment velocity is 128 mm/s, the oil–air meniscus boundary in the entrance region reaches the contact area edge, and the 2137 base oil in the central region experiences significant collapse. When the volume of oil supply is increased to 10 µL, the oil depletion is somehow improved, and at a speed of 256 mm/s, oil film collapse occurs. When the volume of oil supply is increased to 20 µL, no oil depletion occurs at 64 mm/s, and even at a speed of 384 mm/s, the oil–air meniscus boundary in the entrance region does not reach the contact area edge. The interferograms of 2137s are shown in Figure 8b, from which we can see that, under the same test conditions, the inlet oil pool of 2137s is more than that of 2137. The oil–air meniscus boundary of 2137s gradually approaches the contact area edge with increasing speed. It is interesting to find that a larger oil supply quantity results in a more abundant oil pool at the inlet at low speeds. And conversely, with speed increasing, a smaller oil supply quantity leads to a larger distance between the oil–air meniscus boundary and the contact center. That is, there is a more abundant oil supply.

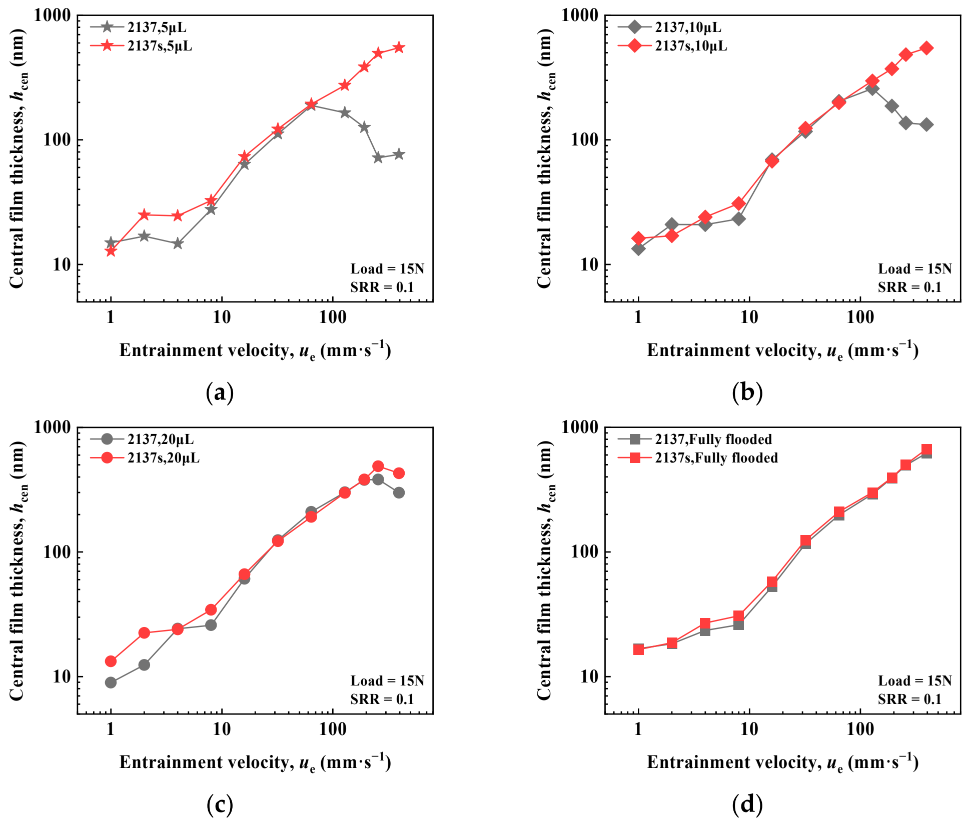

Figure 7. Central film thickness varies with entrainment velocity at different oil supply amounts. (w = 15 N, SRR = 0.1): (**a**) V = 5 μL; (**b**) V = 10 μL; (**c**) V = 20 μL; (**d**) fully flooded.

As shown in Figure 9, the central film thickness of 2137s and base oil 2137 changes with the entrainment velocity under two oil supply quantities. It can be found from the figure that the central film thickness of base oil 2137 increases with the increase of oil supply, which is the same as what we expected. However, when the entrainment velocity is less than 256 mm/s, the central film thickness of 2137s has no obvious difference for the oil supply volumes of 5 μL and that of 10 μL. When the entrainment velocity exceeds 256 mm/s, there is an abrupt film collapse for 10 μL oil supply and, consequently, the film thickness of 5 μL oil supply is much higher than that of 10 μL oil supply, which is beyond our general understanding. This is due to the joint action of centrifugation and adhesion of oil droplets to the surface. More discussions will be given in the subsequent section.

To further explore the influence of stearic acid on the lubricating performance of 2137 base oil under limited lubricant supply conditions, the variation of COF with speed was investigated as shown in Figure 10. The tests were conducted with a load of 15 N and a SRR of 0.1, under 5 μL, 20 μL, and fully flooded conditions for both lubricants. The COFs of 2137 and 2137s both exhibited a decreasing-then-increasing change with increasing speed. Moreover, the COF of 2137s was consistently lower than that of 2137 under all three oil supply amounts, with the difference being most pronounced at low speeds. When the volume of oil supply was 5 μL, the difference in COF between 2137 and 2137s was also significant at low speeds, mainly due to their lubrication states. At high speeds, 2137 exhibited obvious oil depletion, while 2137s maintained better lubrication, resulting in lower COF for 2137s. Furthermore, when the oil supply amount was increased to 20 μL, both 2137 and 2137s showed a significant decrease in COF compared to the 5 μL condition.

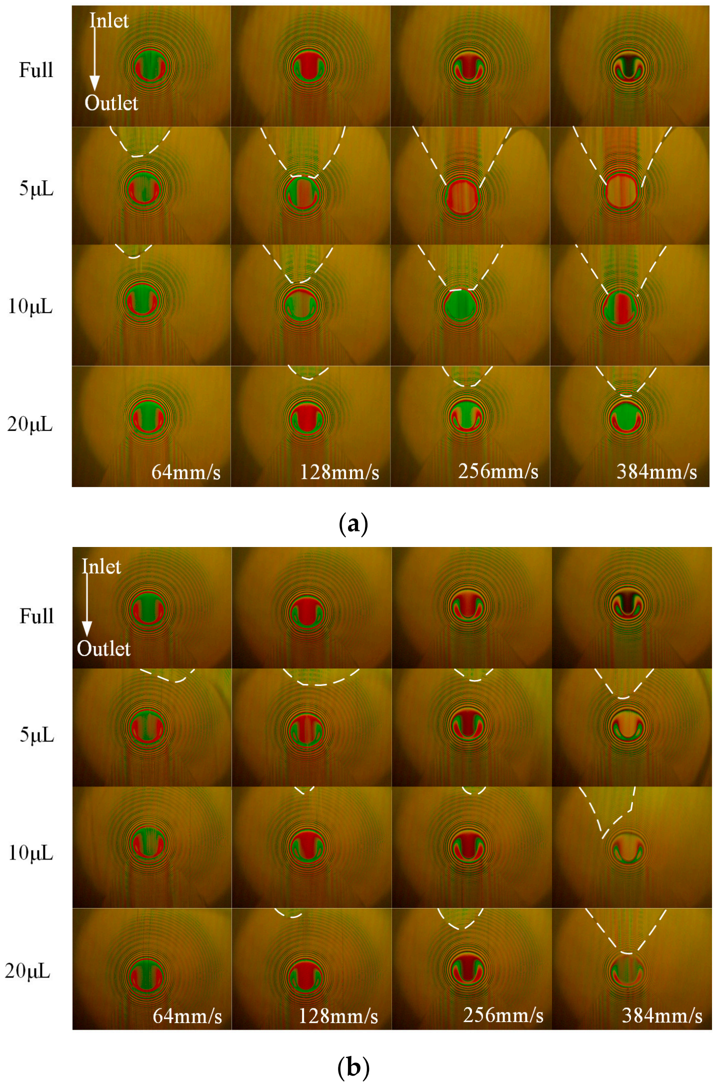

Figure 8. Changes in the oil film interferogram (w = 15 N, SRR = 0.1): (**a**) 2137; (**b**) 2137s.

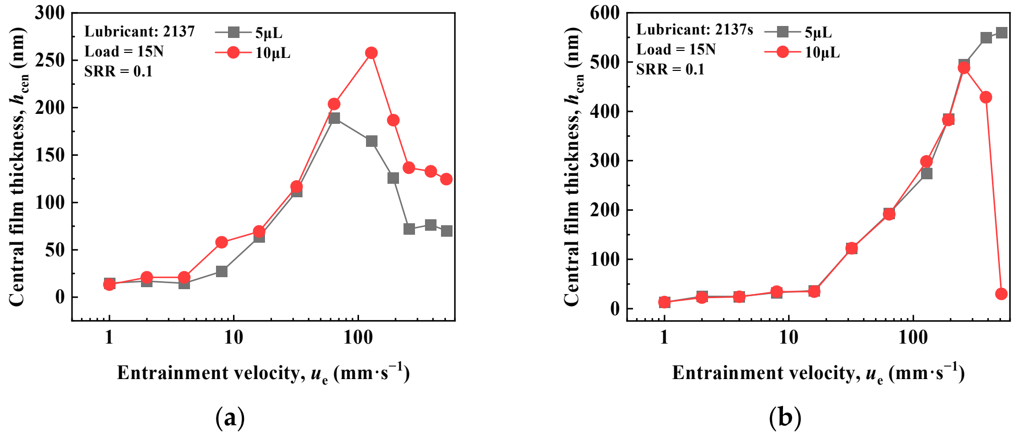

Figure 9. Comparison of center film thickness of 2137s and 2137 base oil under different oil supply conditions: (**a**) central film thickness of 2137; (**b**) central film thickness of 2137s.

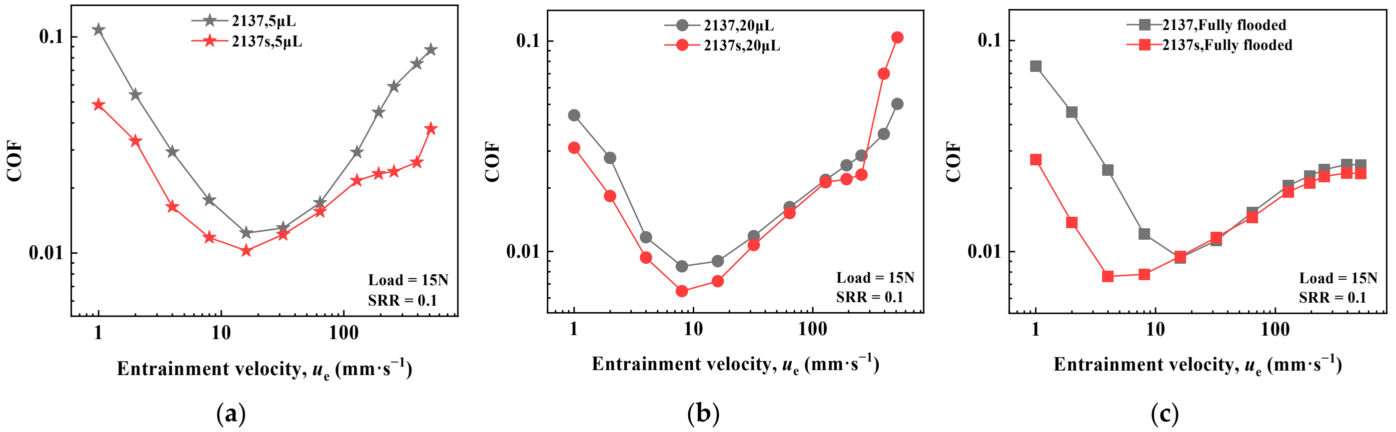

Figure 10. COF vs. entrainment velocity with different oil supply amounts (w = 15 N, SRR = 0.1): (**a**) V = 5 μL; (**b**) V = 20 μL; (**c**) fully flooded.

3.3. Lubrication Mechanism Analysis

The above experimental results show that stearic acid significantly improves the lubricating performance of 2137 base oil as additives, whether under fully flooded or limited lubricant supply conditions. In order to simulate the stearic acid adsorption on tribo-surfaces, adsorption tests were carried out on glass and steel surfaces using 2137s. The glass block and the steel block used in the adsorption tests were the same as those used in the optical EHL experiments. The glass block and steel block were ultrasonically cleaned in petroleum ether and alcohol for 10 min, and then dried. Subsequently, the glass block and steel block were immersed in 2137s for 6 h. After immersion, the block samples were wiped with petroleum ether and alcohol to remove surface lubricant, and contact angle tests were conducted on both the original surface and the treated surface (with 2137s) using 2137 base oil. The results are shown in Figure 11. It can be observed from the figure that the contact angle on the surface of the samples immersed in 2137s is higher than that of the original surface. This indicates that the stearic acid adsorbed on the sample surface changes the surface tension between the solid and liquid interfaces, reducing the surface energy of the tribo-pair contact surface.

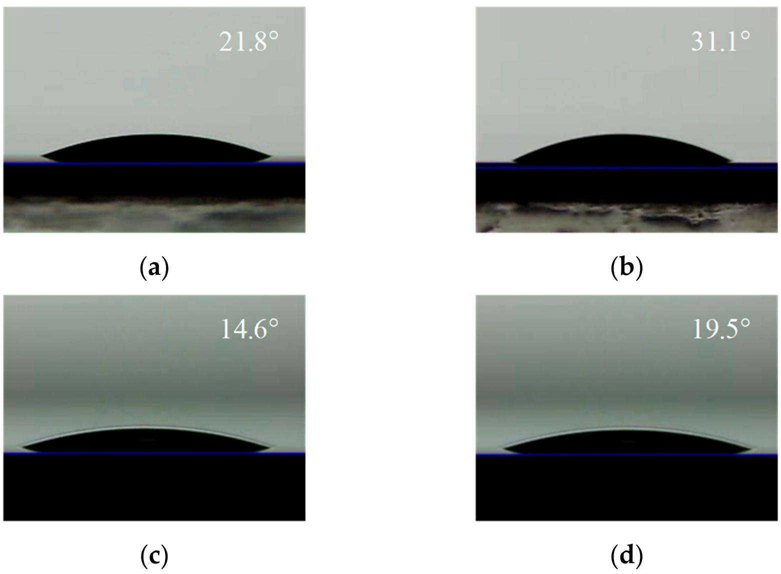

Figure 11. Contact angle of the lubricant on the steel block and glass block: (**a**) original glass block; (**b**) treated glass disc; (**c**) original steel block; (**d**) treated steel block.

Since the adsorption of stearic acid has an influence on the distribution of the oil on the running track, after the tests with a load of 15 N, SRR of 0.1, speed of 10 mm/s, and an oil supply amount of 5 μL, the lubrication tracks of the two lubricants were recorded using a camera. Figure 12a shows the oil distribution patterns of 2137 and 2137s lubricants on the running track of the glass disc, respectively. It can be observed that after the tests, the lubrication track with 2137 exhibited a typical continuous thin oil layer with two side ridges, while 2137s exhibited discrete droplet distribution. The discrete droplet distribution of 2137s on the lubricating track is attributed to the absorbed stearic acid layer on the surface, which has low surface energy and induces the dewetting of oil. Figure 12b shows the distribution of droplets on the glass disc for different oil supply amounts of 2137s. It can be seen clearly that the size of the droplets and their spacing increase with the increase in oil supply amount. When the oil supply amount is 20 μL, the droplets and their spacing become larger. On the other hand, the oil supply amount of 5 μL presents smaller droplet size with less spacing.

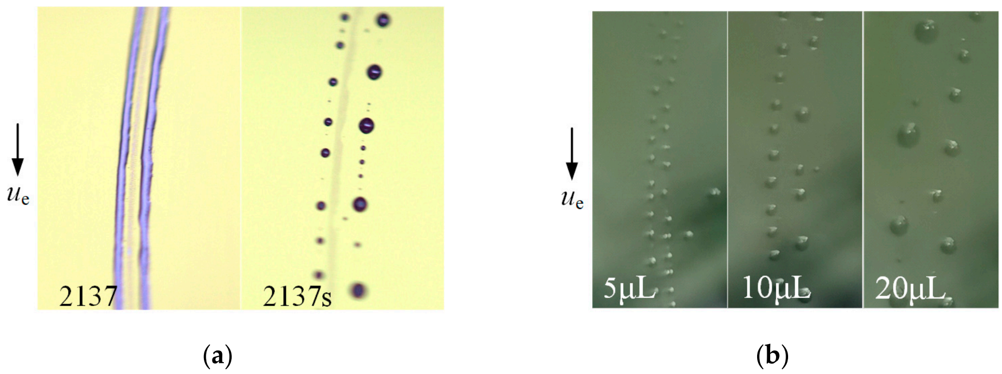

Figure 12. Lubricant distribution on the glass disc: (**a**) the difference between 2137 and 2137s at an oil supply of 5 μL; (**b**) the difference of the volumes of the oil supply with 2137s.

Numerical methods have shown that lubricant supply in the form of droplets is more effective in establishing lubricant film than a uniform oil layer, mainly due to the oil film pressure formed in the early stage when the droplets enter the bearing contact [26]. As shown in Figure 13, the discrete oil droplets can fill the inlet gap, resulting in a larger area of load-bearing and higher induced oil film thickness.

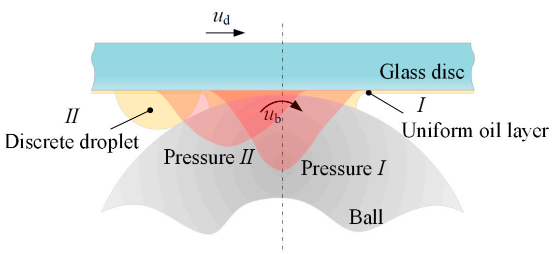

Figure 13. Schematic diagram of oil film pressure for uniform oil layer and discrete oil droplet distribution.

From Figure 12b, we can see that the distribution of 2137s on the lubrication track is different for the oil supply quantities of 5 μL, 10 μL, and 20 μL. When the volume of oil supply is 5 μL, 2137s stays uniformly and densely in the form of small droplets on the lubricating track. Under the conditions of 10 μL and 20 μL oil supply, the oil is distributed sparsely in the form of large droplets on the lubricating track, and most of the oil droplets are kept outside the lubricating track. During the test, due to the rotation of the glass disc, with the increase of entrainment velocity, the centrifugal force effect on the droplet is gradually enhanced, and the droplet has a tendency to leave the lubricating track. For the droplet on the lubricating track, the droplet is subjected to the combination of adhesion and centrifugal force on the surface of the glass disc when the glass is circling. Assuming that the droplet is a spherical crown. The contact angle with the surface of the glass disc is θ. The radius of the bottom circle is r. And when the unit area adhesion force of the solid–liquid interface is constant, the ratio of the adhesion force (F_{adh}) to the centrifugal force (F_{centri}) can be estimated according to Equations (1)–(3).

$$F_{\mathrm{adh}} \propto r^2 \tag{1}$$

$$F_{\mathrm{centri}} \propto r^3 f(\theta) \tag{2}$$

$$\frac{F_{\mathrm{adh}}}{F_{\mathrm{centri}}} = \frac{1}{r} f(\theta) \tag{3}$$

According to Equation (3), the ratio of adhesion force to centrifugal volume force increases with the decrease of droplet size, that is, the centrifugal force per unit volume of droplet is the same. The large droplet will be removed from the lubricating track before the small droplet. It can be seen that due to this scaling effect, the actual oil supply provided by the 5 μL lubricating oil in the aforementioned test is better than that provided by the 10 μL volume lubricant. It should be pointed out that the above analysis is only a conceptual explanation, and theoretical modeling and numerical analysis are needed to describe it quantitatively. Therefore, when the entrainment velocity is higher than 256 mm/s, the central oil film thickness of 5 μL is greater than that of 10 μL.

4. Conclusions

Using the optical interference lubricating film measurement system, experiments were conducted to investigate the effect of stearic acid adsorption on the lubricating performance of mineral oil 2137 under sufficient oil supply and limited lubricant supply conditions. The results can be summarized as follows:

(1) Under conditions of sufficient oil supply, 2137 and 2137s achieve similar oil film thickness, but the COF of 2137s is significantly lower than that of 2137, indicating a weak affinity at the oil film/adsorption layer interface. Overall, the average COF of 2137s is 13.3% smaller than that of 2137.

(2) Under conditions of sufficient oil supply, the SRR has an important influence on the lubricating performance. At a high SRR and high entrainment velocity, the lubricant is prone to thermal thinning, resulting in a significant decrease in COF.

(3) Under conditions of limited lubricant supply, 2137 base oil is prone to oil starvation as the entrainment velocity increases, and the less the oil supply, the earlier the occurrence of oil starvation. Compared to 2137, 2137s significantly improves the oil starvation phenomenon, which is related to the discrete oil distribution due to adsorption of stearic acid on the contact surface.

(4) The adsorption film formed by 2137s on the glass disc surface reduces surface energy, and the lubricating oil with a discrete droplet distribution on the lubricating track due to "dewetting" is beneficial for early load-bearing at the entrance of the contact area, thereby reducing the COF.

(5) With increase in the disc speed, it is interesting to find that less 2137s supply quantity can produce higher film thickness, which can be explained by the fact that a smaller 2137s supply quantity generates droplets with a smaller size, and presents oil with more resistance to the centrifugal force to leave the lubrication track.

Author Contributions: Conceptualization, W.L. and F.G.; methodology, W.L.; validation, Z.M.; investigation, W.L.; resources, W.L.; writing—original draft preparation, W.L.; writing—review and editing, F.G.; supervision, C.L.; funding acquisition, F.G. All authors have read and agreed to the published version of the manuscript.

Funding: This research was funded by the National Natural Science Foundation of China, grant number 52175173 and the 'Taishan Scholar' Talents Project from Shandong province, grant number No. TS20190943.

Data Availability Statement: Not applicable.

Acknowledgments: The authors are so grateful to the valuable suggestion from Xiaoling Liu during the study.

Conflicts of Interest: The authors declare no conflict of interest.

References

1. Yang, P.R. *Numerical Analysis of Fluid Lubrication*; Beijing National Defense Industry Press: Beijing, China, 1998.
2. Cai, X.J.; Liu, Z.Q.; Chen, M.; An, Q.L. An experimental investigation on effects of minimum quantity lubrication oil supply rate in high-speed end milling of Ti–6Al–4V. *Proc. Inst. Mech. Eng. Part B J. Eng. Manuf.* **2012**, *226*, 1784–1792. [CrossRef]
3. Van der Kruk, W.M.; Smit, S.A.; Segers, T.J.; Li, X.M.; Venner, C.H. Drop-on-demand printing as novel method of oil supply in elastohydrodynamic lubrication. *Tribol. Lett.* **2019**, *67*, 95. [CrossRef]
4. Wedeven, L.D.; Evans, D.; Cameron, A. Optical analysis of ball bearing starvation. *J. Tribol.* **1971**, *93*, 349–361. [CrossRef]
5. Guangteng, G.; Cann, P.M.; Spikes, H.A. A study of parched lubrication. *Wear* **1992**, *153*, 91–105. [CrossRef]
6. Kingsbury, E.; Schritz, B.; Prahl, J. Parched Elasto Hydrodynamic Lubrication Film Thickness Measurement in an Instrument Ball Bearing. *Tribol. Trans.* **1990**, *33*, 11–14. [CrossRef]
7. Fischer, D.; Jacobs, G.; Stratmann, A.; Burghardt, G. Effect of base oil type in grease composition on the lubricating film formation in EHD contacts. *Lubricants* **2018**, *6*, 32. [CrossRef]
8. Cann, P.M.E.; Damiens, B.; Lubrecht, A.A. The transition between fully flooded and starved regimes in EHL. *Tribol. Int.* **2004**, *37*, 859–864. [CrossRef]
9. Maruyama, T.; Saitoh, T. Relationship between supplied oil flow rates and oil film thicknesses under starved elastohydrodynamic lubrication. *Lubricants* **2015**, *3*, 365–380. [CrossRef]
10. Ebner, M.; Yilmaz, M.; Lohner, T.; Michaelis, K.; Höhn, B.-R.; Stahl, K. On the effect of starved lubrication on elastohydrodynamic (EHL) line contacts. *Tribol. Int.* **2018**, *118*, 515–523. [CrossRef]
11. Niu, Y.; Pang, X.; Yue, S.; Shangguan, B.; Zhang, Y. The friction and wear behavior of Laser Textured Surfaces in non-conformal contact under Starved Lubrication. *Wear* **2021**, *476*, 203723. [CrossRef]
12. Matthew, H.; Matthew, S.; Ramin, R.; Nekouie-Esfahani, R. Effect of surface texture positioning in grease lubricated contacts. *Tribol. Int.* **2023**, *185*, 108523.
13. Hirayama, T.; Ikeda, M.; Suzuki, T.; Matsuoka, T.; Sawada, H.; Kawahara, K. Effect of nanotexturing on increase in elastohydrodynamic lubrication oil film thickness. *J. Tribol.* **2014**, *136*, 031501. [CrossRef]
14. Li, X.; Guo, F.; Wong, P.; Zhao, Y. Regulation of lubricant supply by wettability gradient in rolling EHL contacts. *Tribol. Int.* **2018**, *120*, 565–574. [CrossRef]
15. Zhao, W.; Wang, L.; Xue, Q. Influence of micro/nano-textures and chemical modification on the nanotribological property of Au surface. *Colloids Surf. A Physicochem. Eng. Asp.* **2010**, *366*, 191–196. [CrossRef]
16. Wen, S.Z.; Huang, P.; Tian, Y.; Ma, L.R. *Principles of Tribology*, 5th ed.; Tsinghua University Press: Beijing, China, 2018.
17. He, X.; Lu, J.; Desanker, M.; Invergo, A.M.; Lohr, T.L.; Ren, N.; Lockwood, F.E.; Marks, T.J.; Chung, Y.-W.; Wang, Q.J. Boundary lubrication mechanisms for high-performance friction modifiers. *ACS Appl. Mater. Interfaces* **2018**, *10*, 40203–40211. [CrossRef]
18. Hu, W.-J.; Xu, Y.; Zeng, X.; Li, J.-S. Alkyl-ethylene amines as effective organic friction modifiers for the boundary lubrication regime. *Langmuir* **2020**, *36*, 6716–6727. [CrossRef]
19. Somayaji, A.; Aswath, P.B. The role of antioxidants on the oxidation stability of oils with F-ZDDP and ZDDP, and chemical structure of tribofilms using XANES. *Tribol. Trans.* **2009**, *52*, 511–525. [CrossRef]
20. Wang, Z.; Chang, J.; Wu, W. Synergistic effects of phosphate ionic liquids and octadecylaminen-oleoyl sarcosinate as lubricating grease additives. *Lubr. Sci.* **2019**, *31*, 127–136. [CrossRef]
21. Faujdar, E.; Negi, H.; Singh, R.K.; Varshney, V. Study on Biodegradable Poly (α-Olefins–co–α-Pinene) Architectures as Pour Point Depressant and Viscosity Index Improver Additive for Lubricating Oils. *J. Polym. Environ.* **2020**, *28*, 3019–3027. [CrossRef]
22. Battez, A.E.H.; González, R.; Viesca, J.L.; Blanco, D.; Asedegbega, E.; Osorio, A. Tribological behaviour of two imidazolium ionic liquids as lubricant additives for steel/steel contacts. *Wear* **2009**, *266*, 1224–1228. [CrossRef]
23. Wells, H.M.; Southcombe, J.E. Theory and Practice of Lubrication. *Sci. Am.* **1920**, *2* (Suppl. 1), 32–36. [CrossRef]
24. Doig, M.; Warrens, C.P.; Camp, P.J. Structure and friction of stearic acid and oleic acid films adsorbed on iron oxide surfaces in squalane. *Langmuir* **2014**, *30*, 186–195. [CrossRef] [PubMed]
25. Ewen, J.P.; Gattinoni, C.; Morgan, N.; Spikes, H.A.; Dini, D. Nonequilibrium molecular dynamics simulations of organic friction modifiers adsorbed on iron oxide surfaces. *Langmuir* **2016**, *32*, 4450–4463. [CrossRef] [PubMed]
26. Fry, B.M.; Moody, G.; Spikes, H.A.; Wong, J.S.S. Adsorption of organic friction modifier additives. *Langmuir* **2020**, *36*, 1147–1155. [CrossRef] [PubMed]

27. Kalin, M.; Kus, M. New strategy for reducing the EHL friction in steel contacts using additive-formed oleophobic boundary films. *Friction* **2021**, *9*, 1346–1360. [CrossRef]
28. Zang, S.Y.; Guo, F.; Li, C. Influence of Surface Wettability on Lubrication by Limited Lubricant Supply. *Tribology* **2017**, *37*, 429–434.
29. Li, S.Y.; Guo, F.; Wong, P.L.; Li, X. Numerical analysis of lubrication of conformal contact with discontinuous oil droplets. *Tribol. Int.* **2022**, *173*, 107632.
30. Liu, H.C.; Guo, F.; Guo, L.; Wong, P.L. A dichromatic interference intensity modulation approach to measurement of lubricating film thickness. *Tribol. Lett.* **2015**, *58*, 1–11. [CrossRef]